Mechanisms of Cardiac Nerve Sprouting After Myocardial Infarction in Dogs

Shengmei Zhou, Lan S. Chen, Yasushi Miyauchi, Mizuho Miyauchi, Saibal Kar, Simon Kangavari, Michael C. Fishbein, Behrooz Sharifi, Peng-Sheng Chen

Abstract—Cardiac nerve sprouting and sympathetic hyperinnervation after myocardial infarction (MI) both contribute to arrhythmogenesis and sudden death. However, the mechanisms responsible for nerve sprouting after MI are unclear. The expression of nerve growth factor (NGF), growth associated protein 43 (GAP43), and other nerve markers were studied at the infarcted site, the noninfarcted left ventricle free wall (LVFW), and the left stellate ganglion (LSG) at several time points (30 minutes to 1 month) after MI. Transcardiac (difference between coronary sinus and aorta) NGF levels were also assayed. Acute MI resulted in the immediate elevation of the transcardiac NGF concentration within 3.5 hours after MI, followed by the upregulation of cardiac NGF and GAP43 expression, which was earlier and more pronounced at the infarcted site than the noninfarcted LVFW. However, cardiac nerve sprouting and sympathetic hyperinnervation were more pronounced in the noninfarcted than the infarcted LVFW site and peaked at 1 week after MI. The NGF and GAP43 protein levels significantly increased in the LSG from 3 days ($P<0.01$ for all) after MI, without a concomitant increase in mRNA. There was persistent elevation of NGF levels in aorta and coronary sinus within 1 month after MI. We conclude MI results in immediate local NGF release, followed by upregulation of NGF and GAP43 expression at the infarcted site. NGF and GAP43 are transported retrogradely to LSG, which triggers nerve sprouting at the noninfarcted LVFW. A rapid and persistent upregulation of NGF and GAP43 expression at the infarcted site underlies the mechanisms of cardiac nerve sprouting after MI. **(*Circ Res*. 2004;95:000-000.)**

Key Words: nerve growth factor ■ nerve sprouting ■ sympathetic nerve ■ ventricular arrhythmia

We previously demonstrated that heterogeneous cardiac nerve sprouting and sympathetic hyperinnervation play important roles in arrhythmogenesis and sudden cardiac death in both human patients and animal models of myocardial infarction (MI).[1–6] However, the mechanisms and time course of nerve sprouting after MI are unclear. Nerve growth factor (NGF) is a neurotrophin that supports the survival and differentiation of sympathetic neurons and enhances target innervation.[7,8] NGF also regulates the synthesis of neurofilament and tubulin proteins, promotes Schwann cell migration,[9] modulates synaptic transmission between sympathetic neurons and cardiac myocytes,[10] and increases the half-life of growth associated protein-43 (GAP43).[11] Overexpression of NGF within the heart of transgenic mice causes hyperinnervation.[12] Peripheral nerve injury results in increased local NGF expression, which facilitates nerve regeneration.[13] It is possible that increased NGF expression also underlies the mechanisms of cardiac nerve sprouting after ischemic injury and MI. In the present study, we sampled blood and harvested tissues from the left ventricle and from the left stellate ganglion at different time points after experimental canine MI. NGF expression and the magnitude of cardiac nerve sprouting were studied to test the hypothesis that increased local NGF production underlies the mechanisms of nerve sprouting after MI.

Materials and Methods

The animal experiments were performed with approval of the Institutional Animal Care and Use Committee of the Cedars-Sinai Medical Center. Mongrel dogs (22 to 28 Kg) were obtained from a USDA licensed commercial dog vendor in Missouri. Propofol and isoflurane were used for general anesthesia during all surgical procedures.

Surgical Procedure

MI was created by ligating the left anterior descending coronary artery below its first diagonal branch in 14 open-chest and anesthetized dogs.[2] One concern of open-chest ligation is that the ligation itself might directly result in cardiac nerve injury. To address this issue, we created MI in an additional 7 dogs using continuous intracoronary balloon inflation for 1 to 3 hours to occlude blood flow. ECG was monitored to document ST segment elevation. Blood was drawn from the aorta and coronary sinus (CS) simultaneously at baseline, and then at 0.5, 1.5, 2.5, and 3.5 hours after MI. Dogs were followed up 3.5 hours (n=3), 3 days (n=5), 1 week (n=10), and 1 month (n=3) after MI. The 3-day group included 2 dogs with balloon inflation and 3 dogs with epicardial ligation. The 1-week

Original received January 6, 2004; revision received April 29, 2004; accepted May 14, 2004.

From the Division of Cardiology, Department of Medicine (S.Z., Y.M., M.M., S Kar, S Kangavari, B.S., P.-S.C.), Cedars-Sinai Medical Center; the Department of Neurology (L.S.C.), Childrens Hospital and the Keck School of Medicine, University of Southern California; and Division of Anatomical Pathology, Department of Pathology (M.C.F.), David Geffen School of Medicine, UCLA, Los Angeles, Calif.

Correspondence to Peng-Sheng Chen, MD, Room 5342, CSMC, 8700 Beverly Blvd, Los Angeles, CA 90048-1865. E-mail chenp@cshs.org

Circulation Research **is available at http://www.circresaha.org** **DOI: 10.1161/01.RES.0000133678.22968.e3**

Primer Sequence and Amplicon Size of Genes Validated by Taqman RT-PCR

Gene Name	Accession No.	Primer Sequence	Amplicon Size, bp
NF	AF346625	F: 5′-CCAGGCGATGGACAATTATGTT-3′	55
		R: 5′-GCATATATCACATTCGGCTACGTAA-3′	
NGF	M57399	F: 5′-GCGGAGTGCAAATACCAGTTC-3′	56
		R: 5′-AGGGCTGTGTTCAGGTCACAT-3′	
GAP43	BI395915	F: 5′-CAAGATGGCATCAAACCAGAAG-3′	51
		R: 5′-CACGGAAGCTAGCCTGAATTTT-3′	
SYN	BQ091719	F: 5′-AGCGTGGAGTGTGCCAACA-3′	101
		R: 5′-CAGGTGGGTGCATCAAAGTACA-3′	
GAPDH	AB038240	F: 5′-AAAGCTGCCAAATATGACGACAT-3′	51
		R: 5′-CTCCGATGCCTGCTTCACTAC-3′	

NF indicates neurofilament; SYN, synaptophysin.

group included a subgroup of 5 dogs with intracoronary balloon inflation and another subgroup of 5 dogs with epicardial ligation. We performed a second surgery at the end of the followup, and ECG and blood samples were obtained again. Fresh cardiac tissue from the infarcted site, noninfarcted left ventricle free wall (LVFW), and left stellate ganglion (LSG) were sampled using sharp skin biopsy punches (Acu-Punch, Acuderm Inc)[15] and a scalpel. The samples were immediately frozen in liquid nitrogen and stored in −80°C for further processing. Two corresponding sites from left ventricle and LSG were sampled from the control group. The hearts were then excised and immersed in 4% formalin for 1 hour, followed by storage in 70% alcohol for immunohistological study. Infarct size was determined as previously reported.[2]

mRNA Analyses

Total RNA was extracted from the infarcted site, noninfarcted LVFW, and LSG using TRIZOL (Invitrogen) according to the manufacturer's protocol, treated with Dnase I (Qiagen) to degrade any trace of DNA, and later cleaned again with Rneasy Kit (Qiagen). The integrity of each sample was confirmed by analysis on an agarose gel. Total RNA was reversely transcripted using reverse transcription reaction with TaqMan Reverse Transcription Reagents (Applied Biosystems). The expression levels of candidate genes were measured by real-time quantitative RT-PCR (qRT-PCR) using SYBR Green PCR Master mix (Applied Biosystems) and primer pairs specific for canine on an ABI PRISM 7700 Sequence Detection System (Applied Biosystems) according to the manufacturer's protocol. The cycle at which the amplification plot crosses the threshold is known to accurately reflect relative mRNA values.[16] In each assay, both glyseraldehyde-3-phosphate dehydrogenase (GAPDH, used as endogenous control) and target gene from the same samples were amplified in duplicate in separate tubes. mRNA levels of each gene were calculated using the relative standard curve method and normalized against corresponding GAPDH mRNA level, and then expressed as relative change over control±SD. A single dissociation peak was detected in each reaction by the dissociation curve. The expected size amplicons were confirmed by gel electrophoreses. The sequences of the genes studied were obtained from GenBank, and the primers were designed using the Primer Express software (Applied Biosystems). The Table shows the primer sequence and amplicon size of the selected genes.

Western Blotting Studies

Cardiac tissues and the remaining LSG were homogenized on ice with cell lysis buffer (Cell Signaling Technology), and supernatants were collected as total lysate. Equal amounts (60 μg) of denatured proteins were fractionated on 4% to 20% Gradient Minigel (CPL) and transferred to PVDF membranes (Bio-Rad). The membranes were blocked with 5% nonfat dry milk in PBST (containing 0.05% Tween 20), and incubated overnight at 4°C with the primary antibody (NGF, 1:200, Santa Cruz Biotechnology; GAP43, 1:1000 and tyrosine hydroxylase (TH), 1:500; Chemicon), washed in PBST, incubated with horseradish peroxidase–conjugated second antibody, and revealed by Immun-Star HRP Substrate (Bio-Rad). For normalization of gel loading, the same Western blots were reprobed with anti-GAPDH at 1:10 000 dilution (Research Diagnostics Inc). The density of bands on Western blots was quantified by the use of Kodak imaging station systems.

Immunohistochemical Studies

Samples were taken from the infarcted site and noninfarcted LVFW and routinely processed. Sections (5 μm thick) were mounted on charged slides. A modified immunohistochemical ABC method was used for immunostaining for GAP43 (a marker of nerve sprouting), TH, and neurofilament (markers of sympathetic nerves).[2] The density of stained nerves was determined using ImagePro software and expressed as the nerve area divided by the total area examined ($\mu m^2/mm^2$).[5] The investigators were blinded to the specimen's source. The nerve density of each slide was determined by the average of 3 fields with the highest nerve density.

Enzyme-Linked Immunosorbent Assay

Serum NGF concentrations were assayed by sandwich enzyme-linked immunosorbent assay (ELISA) using NGF Emax Immuno-Assay System (Promega) according to the manufacturer's instructions. All assays were performed on F-bottom 96-well plates (Nunc). Tertiary antibodies were conjugated to horseradish peroxidase. Wells were developed with tetramethylbenzidine and measured at 450 nm. NGF content was quantified against a standard curve calibrated with known amounts of protein. All samples were assayed in triplicate and expressed as a mean. Transcardiac NGF concentration is defined by the difference of NGF concentrations in the CS and aorta.

Statistical Analyses

The Student *t* tests were used to compare the means. ANOVA with Newman-Keuls test was used for multiple comparisons. A value of $P \leq 0.05$ was considered significant.

Results

Characterization of the MI Dogs

During first surgery, ST segment elevation and frequent premature ventricular contractions (PVCs) were observed immediately after the induction of MI in all dogs. Short nonsustained ventricular tachycardia (VT) was observed in 11/21 dogs. Three dogs were euthanized during first surgery, after blood samples were obtained 3.5 hours after MI. All remaining 18 dogs survived during follow-up. During second surgery, we observed ST segment elevation in 18/18, PVC in

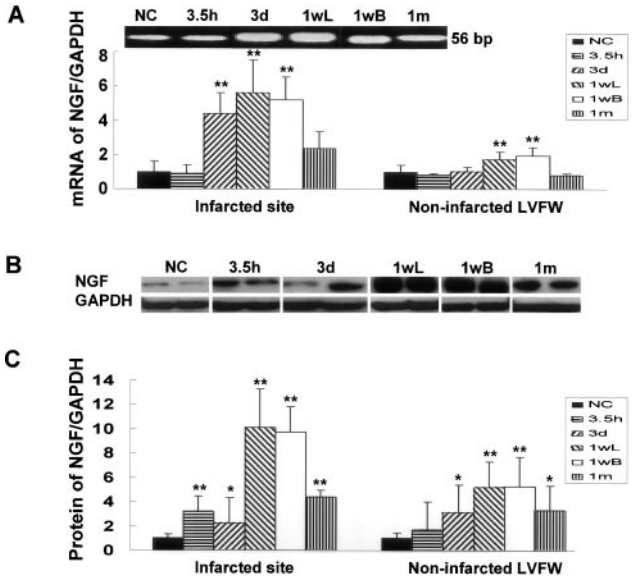

Figure 1. NGF mRNA and protein levels at different time points and regions of heart after MI (GAPDH normalized, arbitrary units). A, Representative qRT-PCR products at the infarcted site (top) and the relative NGF mRNA expression levels. B, Representative Western blotting bands of NGF at the infarcted site. Bands of GAPDH were shown to demonstrate protein loading of each lane. C, Quantitation of autoradiographic signals of Western blots. 1wL indicates ligation group at 1 week; 1wB, balloon occlusion group at 1 week. *$P<0.05$; **$P<0.01$ vs normal control (NC).

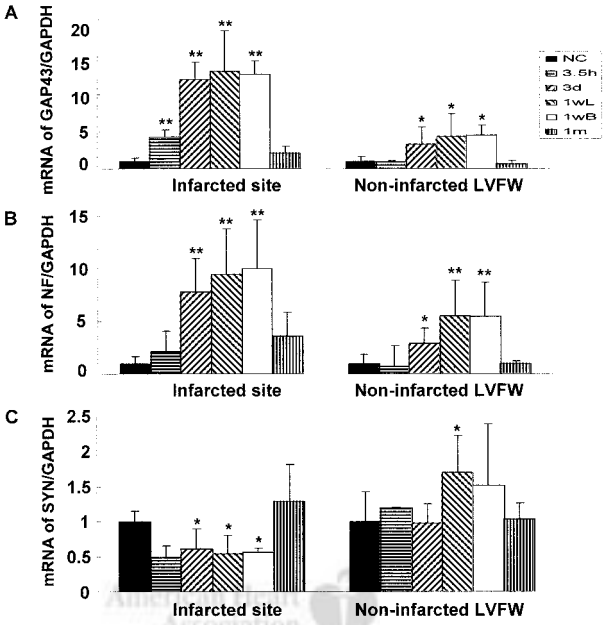

Figure 2. mRNA levels of GAP43, neurofilament (NF), and synaptophysin (SYN) at different time points at both the infarcted site and noninfarcted LVFW (GAPDH normalized, arbitrary units). GAP43 mRNA level progressively increased at the infarcted site from 3.5 hours to 1 week, to a lesser extent at the noninfarcted LVFW. Similar to GAP43 expression pattern, NF mRNA significantly increased at 3 days and 1 week at both sites. However, synaptophysin significantly decreased at 3 days and 1 week at the infarcted site but increased at the noninfarcted LVFW at 1 week in the ligation group. 1wL indicates ligation group at 1 week; 1wB, balloon occlusion group at 1 week. *$P<0.05$; **$P<0.01$ vs NC.

9/18, and nonsustained VT in 3/18 dogs. The average MI size was 14.1±4.6%.

Heterogeneous Cardiac NGF Expression After MI

To study the temporal and spatial variation of NGF expression after MI, we analyzed NGF mRNA levels at the infarcted site and noninfarcted LVFW at 3.5 hours, 3 days, 1 week, and 1 month after MI by using real-time qRT-PCR. The specificity of amplified PCR product was verified by agarose gel electrophoresis (Figure 1A, top panel). Nonspecific DNA fragments were not detected. The relative NGF mRNA levels at different time points and locations of heart were shown in Figure 1A. At 3.5 hours after MI, the NGF mRNA levels at both the infarcted site and noninfarcted LVFW were not significantly different from the control group. At 3 days after MI, the infarcted site but not noninfarcted LVFW showed significant increase in NGF mRNA compared with the control group (4.4-fold, $P<0.01$). At 1 week after MI, NGF mRNA at both the infarcted site (ligation group, 5.6-fold; balloon group, 5.2-fold) and noninfarcted LVFW (ligation group,1.74-fold; balloon group, 1.96-fold) were significantly increased ($P<0.01$ for both). At 1 month after MI, neither location showed significant changes in NGF expression (P=NS). In general, the upregulation of NGF mRNA expression was earlier and more pronounced at the infarcted site than the noninfarcted LVFW.

To confirm qRT-PCR results, we performed Western blotting with an NGF antibody. Figure 1B shows representative bands (26 kDa) from a gel on which NGF protein at the infarcted site was studied. The GAPDH bands used to confirm equal loading were of similar density. Weak NGF protein was expressed in the myocardium of normal hearts. At the infarcted site, the NGF bands in the MI group were consistently denser and wider than those of the control group. Densitometric data showed that NGF protein levels were significantly higher in the MI group than they were in the control at all time points (2.2- to 10-fold; Figure 1C). At the noninfarcted LVFW, NGF increased 3 days after MI and peaked at 1 week (ligation group, 5.2-fold; balloon group, 5.3-fold; Figure 1C). Similar to qRT-PCR results, NGF protein increased earlier and by a greater magnitude at the infarcted site compared with the noninfarcted LVFW. These data suggest that MI induced immediate local NGF release followed by local NGF production. There was a delay in upregulation of NGF mRNA expression at the noninfarcted LVFW compared with the infarcted site.

Heterogeneous Cardiac GAP43 Expression After MI

The membrane phosphoprotein GAP43 expressed in the growth cones of sprouting axons is a marker for nerve sprouting.[17] We studied GAP43 mRNA expression by real-time qRT-PCR. As shown in Figure 2A, GAP43 mRNA at the infarcted site showed significant increase (4.3-fold, $P<0.01$) at 3.5 hours after MI but not the noninfarcted LVFW. Both the infarcted site (12- to 13-fold, $P<0.01$) and noninfarcted LVFW (3- to 4-fold, $P<0.05$) showed signifi-

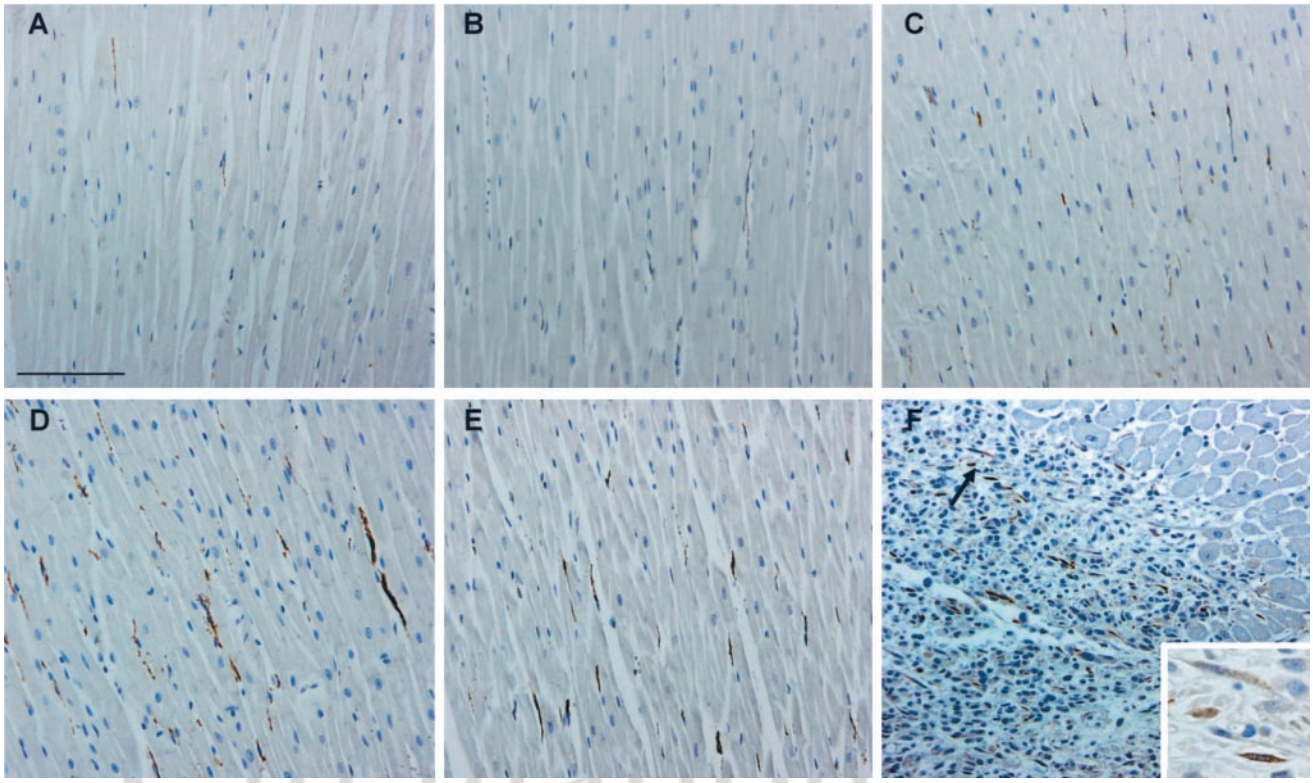

Figure 3. Examples of GAP43 immunostaining. A through E, Noninfarcted LVFW at different time points. A, Control; B, 3.5 hours after MI; C, 3 days after MI; D, 1 week after MI; E, 1 month after MI. Positive staining was marked by brown color. GAP43-positive staining was markedly increased 3 days after MI, and reached a peak at 1 week after MI. F, Example of GAP43 staining at the infarcted site at 1 week. GAP43-positive nerve twigs and stromal cells (see insert, 100× objective) also peaked at 1 week at the infarcted site. Magnification of objective lens (excluding insert in F): 20×. Scale bar=100 μm.

cant increase in GAP43 mRNA at 3 days and 1 week after MI. Similar to the NGF expression pattern, the GAP43 mRNA levels of both sites returned to the control levels at 1 month after MI, and GAP43 mRNA increased earlier and was more pronounced at the infarcted site than the noninfarcted LVFW.

Gene Expression of Other Nerve Specific Markers

We also assayed the mRNA expression of nerve-specific markers neurofilament (an intermediate filament in soma and neuron processes) and synaptophysin (a marker for synaptogenesis) by using real-time qRT-PCR. At 3.5 hours after MI, there were no significant changes in either neurofilament or synaptophysin expression. At 3 days and 1 week after MI, the mRNA levels of neurofilament showed significant increase at both sites compared with the control group (Figure 2B). The mRNA levels of synaptophysin decreased at the infarcted site at 3 days and 1 week after MI and increased at the noninfarcted LVFW at 1 week after MI in the ligation group (Figure 2C). At 1 month after MI, both neurofilament and synaptophysin mRNA returned to control levels. These data imply that MI induced neurofilament expression and inhibited synaptophysin expression at the infarcted site. Because canine-specific TH gene sequence is not available, we could not evaluate TH mRNA.

Nerve Sprouting and Sympathetic Hyperinnervation After MI

Immunohistochemical staining showed few GAP43-positive nerves in the normal LVFW and the noninfarcted LVFW at 3.5 hours after MI (Figure 3A and 3B), but abundant GAP43-positive nerve fibers were observed at the noninfarcted LVFW at 3 days, 1 week, and 1 month after MI (Figure 3C through 3E, respectively). At 3 days after MI, coagulation necrosis of myocardium distal to ligation was evident, with sarcolemmal disruption, hypereosinophilia of fibers and nucleus dropout. At 1 week after MI, inflammatory cells and fibroblastic proliferation were observed in large numbers at the infarcted site. In addition to GAP43-positive nerves, we also observed GAP43-positive stromal cells. These stromal cells, which contained nuclei and appeared around 3 days after MI,[18] were also observed at the infarcted site (Figure 3F). GAP43-positive nerve numbers reached a peak at 1 week after MI at both the noninfarcted LVFW (Figure 3D) and infarcted site (Figure 3F). Although there was much higher GAP43 mRNA expression at the infarcted site than the noninfarcted LVFW, overall GAP43-positive nerve density was lower at the infarcted site than the noninfarcted LVFW. GAP43-positive nerve density in the noninfarcted LVFW was significantly ($P<0.05$ for all) higher in the MI group than the control group at 3 days, 1 week, and 1 month after MI (Figure 4A).

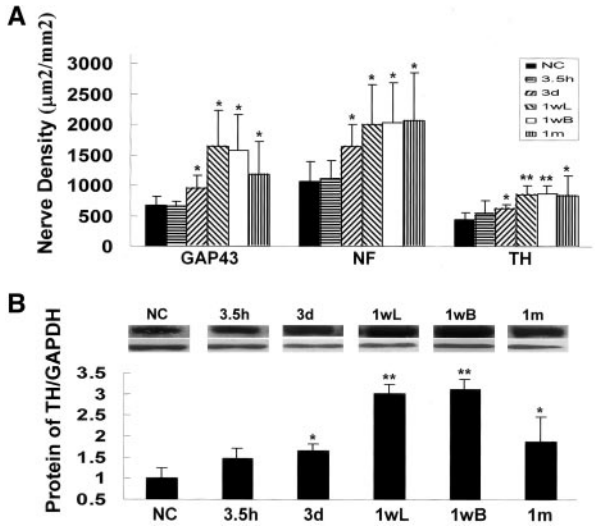

Figure 4. Evolution of sympathetic nerve density and TH protein levels after MI. A, Graphs show GAP43-, neurofilament (NF)-, and TH- positive nerve density at the noninfarcted LVFW at different time points. Nerve densities of all three staining were significantly higher in the MI group than the control group after 3 days, reached a peak at 1 week. B, Western blotting analysis of TH at the noninfarcted LVFW at different time points. Top, Representative Western blots of TH (around 60 kDa). Middle, Corresponding Western blots of GAPDH. Bottom, TH protein levels were much higher in the MI group than the control group at 3 days, 1 week, and 1 month. 1wL indicates ligation group at 1 week; 1wB, balloon occlusion group at 1 week. $^{*}P<0.05$; $^{**}P<0.01$ vs NC.

The positive TH and neurofilament staining patterns were similar to GAP43 staining pattern. Quantitative data showed that the densities of nerves positive for neurofilament and TH were also significantly ($P<0.05$ for all) higher in the MI group than the control group at 3 day, 1 week, and 1 month (Figure 4A). Similar to TH staining results, Western blotting for TH protein at the noninfarcted LVFW showed a significant increase in TH levels in the MI group than the control group, and this increase peaked at 1 week (3-fold, $P<0.01$; Figure 4B). The TH-positive staining of normal control (Figure 5A) was less than that of 3 days, 1 week, and 1 month after MI at the noninfarcted LVFW (Figure 5B through 5D, respectively). The peak density occurred at 1 week after MI. Figure 5E shows neurofilament staining at the infarcted site at 1 week after MI. There were large numbers of nerves and inflammatory cells. Even higher densities of neurofilament-positive nerves were observed at the noninfarcted LVFW. Figure 5F shows diffuse and thin TH-positive nerves at the infarcted site at 1 month after MI. Diffuse intrinsic cardiac adrenergic cells[19] were also observed (insert of Figure 5F). These cells are typically around 5 to 10 μm in diameter, round, and have TH-positive cytoplasm.

Time Course of NGF and GAP43 Expression in the LSG After MI

NGF protein level significantly increased in the LSG 3 days after MI, peaked at 1 week, and was paralleled by a similar increase in GAP43 protein (Figure 6A). However, real-time qRT-PCR results showed no significant change in NGF mRNA levels over time (Figure 6B). Similarly, there was no significant change in the mRNA levels of GAP43 and neurofilament in the MI group compared with the control group (Figure 6B).

Time Course of Transcardiac NGF Level After MI

Transcardiac NGF (Figure 7) increased immediately after MI and peaked at 3.5 hours ($P<0.01$). Serum NGF (both CS and aorta) continued to increase at 3 days (CS by 10±10% and aorta by 10±15%), 1 week (CS by 22±37% and aorta by 20±37% in the ligation group, and CS by 25±35% and aorta by 21±40% in the balloon group), and 1 month (CS by 21±36% and aorta by 18%±36%) after MI compared with baseline. However, because both the CS and aortic NGF increased to a similar extent, the transcardiac NGF levels from 3 days to 1 month were not significantly different from baseline. There were significant variations of systemic NGF levels among dogs (range, 200 to 1100 ng/mL).

Discussion

We found that acute MI resulted in the immediate elevation of transcardiac NGF concentration, probably due to release of NGF from damaged cells within the heart. This was followed by upregulation of cardiac NGF and GAP43 expression that was more pronounced at the infarcted site than the noninfarcted LVFW. The NGF and GAP43 protein also increased in the LSG, without a concomitant increase in mRNA levels. These latter data suggest that the increased NGF and GAP43 in the LSG is due to retrograde axonal transport from the infarcted site.[20–22] The nerve sprouting signal from the LSG triggers a generalized increase in cardiac nerve density throughout the heart, but more so at the noninfarcted LVFW than the infarcted site. The increased neurofilament and synaptophysin expression further confirms cardiac nerve growth activity. Cardiac nerve sprouting and sympathetic hyperinnervation persisted beyond the first week after MI, supported in part by increased systemic NGF concentration. Large interindividual differences were observed in systemic serum NGF concentration, suggesting individual differences in genetic control of cardiac nerve density and magnitude of nerve sprouting after ischemic injury.

NGF Expression After MI

NGF is expressed in heart and other sympathetic targets.[20,21] The production of NGF in target organs determines the density of innervation by the sympathetic nervous system.[23] NGF is known to enhance reinnervation of surgically denervated canine heart.[24] Hiltunen et al[25] demonstrated in rat hearts that NGF mRNA levels at the border zone increased 2- to 4-fold between 2 hours and 120 hours of reperfusion after MI. In the present study, we found that both NGF protein level and mRNA level increased at the infarcted site and noninfarcted LVFW after MI, but earlier and more pronounced at the infarcted site than the noninfarcted LVFW, and that cardiac NGF mRNA expression was dynamic and temporary. Furthermore, we found that transcardiac NGF concentration increased immediately after MI before detectable elevation of cardiac NGF mRNA, implying that immediate transcardiac NGF increase is the result of cardiac NGF release rather than production. Although there was a signifi-

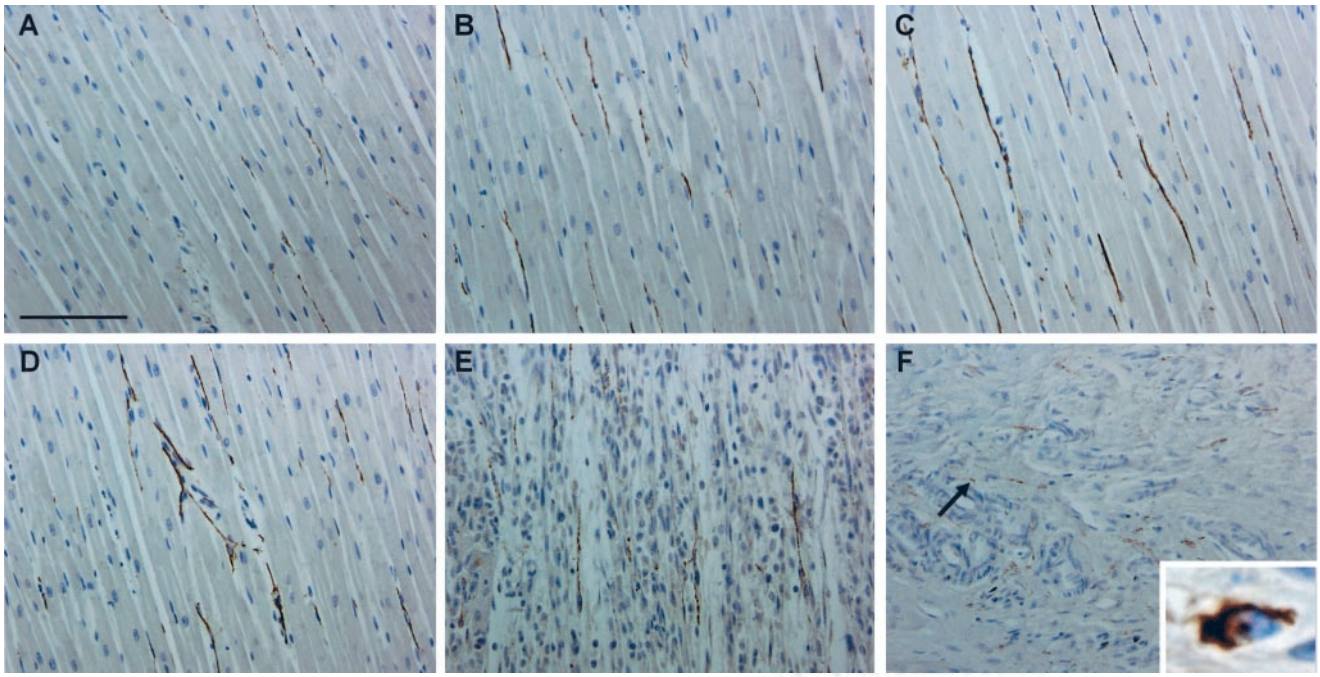

Figure 5. Examples of TH immunostaining. A through D, Noninfarcted LVFW at different time points. A, Control; B, 3 days after MI; C, 1 week after MI; D, 1 month after MI. There were more TH-positive nerves at 3 days, 1 week, and 1 month after MI compared with control, peaking at 1 week. E, Example of neurofilament staining at the infarcted site at 1 week after MI, showing increased numbers of nerves. F, Example of TH staining at the infarcted site at 1 month, showing hyperinnervation and neovascularization. Positive staining pattern (diffuse and thin) of the infarcted site is different from that of noninfarcted LVFW (B through D). Intrinsic cardiac adrenergic cells were also observed (see insert, 100× objective). Magnification of objective lens: 20×. Scale bar=100 μm.

cant increase in NGF protein levels in the LSG from 3 days to 1 month after MI, no significant mRNA increase was observed throughout the study. This suggests that the higher levels of NGF in the sympathetic ganglia result from retrograde axonal transport rather than local synthesis. The observation was compatible with previous studies,[20,21] that demonstrated that superior cervical ganglia contained highest levels of NGF, but its mRNA was barely detectable. We have previously found that nerve sprouting activity in the LSG resulted in generalized nerve sprouting throughout the heart, including both ventricles and atria.[2,3] Putting these observations together, we conclude that MI first induces local NGF release, followed by local NGF production and retrograde transport of NGF to the LSG, which subsequently triggers cardiac nerve sprouting. The observation of nerve sprouting at areas local and remote from the site of insult can be explained by the fact that the LSG and thoracic ganglia innervates the heart globally. Although transcardiac NGF levels returned to normal 3.5 hours after MI, systemic NGF levels continued to increase progressively while cardiac NGF mRNA and protein remained elevated. One possible expla-

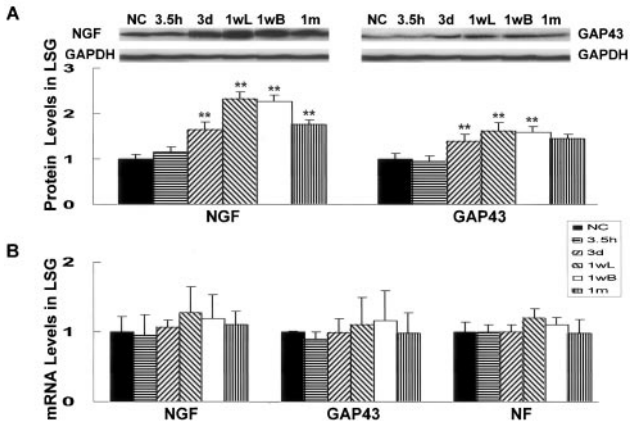

Figure 6. Protein and mRNA levels of NGF and GAP43 in the LSG at different time points (GAPDH normalized, arbitrary units). A, top, Representative Western blots of NGF (left), GAP43 (right), and GAPDH. Bottom, Both NGF and GAP43 protein levels were significantly higher in the MI group than the control group at 3 days, 1 week, and 1 month (**$P<0.01$). B, Relative mRNA levels of NGF, GAP43, and neurofilament (NF). There were no significant changes in these three genes in the MI group compared with the control group at any time points.

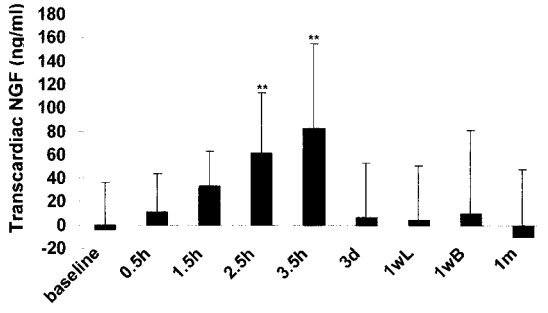

Figure 7. Time course of transcardiac NGF change after MI. Transcardiac NGF at baseline (n=25), 0.5 hours (n=20), 1.5 hours (n=20), 2.5 hours (n=20), 3.5 hours (n=20), 3 days (n=5), 1wL (n=5), 1wB (n=5), and 1 month (n=3) are shown in this figure. MI results in a progressive increase in transcardiac NGF level in 3.5 hours after MI. 1wL indicates ligation group at 1 week; 1wB, balloon occlusion group at 1 week. **$P<0.01$ vs baseline.

nation for this discrepancy is that multiple recirculations of NGF minimized the transcardiac difference of NGF levels. A second explanation is that MI triggers NGF production at extracardiac locations, resulting in an elevation of systemic NGF concentration. We also observed that baseline NGF levels were highly variable between dogs, implying large individual differences in constitutive NGF production. These large individual differences of NGF concentration could result in differential cardiac innervation after MI.

GAP43 and Mechanisms of Cardiac Nerve Sprouting After MI

Our previous study showed that NGF infusion to the LSG induces significant increase in GAP43-positive nerves in the heart.[2] In this study, we found a significant temporal and spatial correlation between cardiac NGF protein level and GAP43 expression. Increased GAP43 protein levels were also observed in LSG from 3 days to 1 month after MI with no significant mRNA increase. This implies that the higher levels of GAP43 in the sympathetic ganglia result from retrograde axonal transport rather than local synthesis, consistent with previous finding that GAP43 is bidirectionally transported in neurons of normal sciatic nerves.[22] GAP43 is a major protein kinase C substrate of growth cones and developing nerve terminals. In the growth cone, it accumulates near the plasma membrane, where it associates with the cortical cytoskeleton and membranes. It is expressed not only in sympathetic nerves but also in parasympathetic and sensory fibers, in certain central nervous system glia, Schwann cell precursors, and nonmyelinating Schwann cells.[26] GAP43 itself enables neurons to sprout new terminals. GAP43 overexpression in transgenic mice leads to the spontaneous formation of new synapse and enhanced sprouting after injury.[27] In the absence of GAP43, growth cones adhered poorly, and failed to produce NGF-induced spreading or insulin-like growth factor-1–induced branching.[28] These observations suggest that NGF may increase cardiac nerve sprouting via upregulation of GAP43 expression. We also observed that although NGF and GAP43 expression levels increased more at the infarcted site than the noninfarcted LVFW, there were less GAP43-positive nerves at the infarcted site than the noninfarcted LVFW. This implies that in addition to neurotrophic factors like NGF and GAP43, nerve sprouting requires a permissive local environment in which to occur. The lack of blood supply at the infarcted site, for example, might impede nerve growth.

Source of mRNA

Although MI resulted in increased NGF, GAP43, and neurofilament mRNA at the infarcted site and noninfarcted LVFW, the source of the mRNA is unclear. It is unlikely that the mRNA came from extracardiac sympathetic ganglia, as the mRNA levels in the LSG were not significantly increased. The most likely source of mRNA is nonneuronal cells near the site of ischemic injury. These nonneuronal cells, including but not limited to the cells that ensheathe nerve fibers, express NGF after transection of the sciatic nerve.[29] Schwann cells are also known to express GAP43 after nerve transaction.[30] Compatible with these findings, we observed GAP43-positive cells within the infarcted site. Some of these cells are stromal cells that are often found in the infarcted myocardia.[18] These nonneuronal cells are the likely source of mRNA detected in this study. A second possible source of mRNA is intrinsic cardiac adrenergic cells.[19] These cells are small TH-positive cells found mostly around blood vessels, with diameters roughly half that of myocytes. These cells could serve as sources of TH. It is also possible that MI can trigger the expression of other neurotrophic mRNAs in these cells.

Limitations

An association between increased NGF expression and sympathetic hyperinnervation does not directly prove a causal relationship. However, our previous study[2] showed that NGF infusion to the LSG can cause significant cardiac nerve sprouting even in normal dogs. These latter findings support a potential cause and effect between elevated NGF in the LSG and cardiac nerve sprouting.

Conclusions

We conclude that MI results in immediate local NGF release, followed by upregulation of NGF and GAP43 expression from nonneuronal cells at the infarcted site. NGF and GAP43 are transported retrogradely to the LSG, which triggers nerve sprouting at the noninfarcted LVFW and, to a lesser degree, the infarcted site. Individual differences of NGF expression might be partially responsible for differential nerve sprouting and susceptibility to arrhythmia after MI. The timely regulation of NGF and GAP43 expression after MI might provide a novel opportunity for arrhythmia control.

Acknowledgments

This study was supported by a NASPE Michel Mirowski International Fellowship and AHA Western Region Fellowship (S.Z.); a Piansky endowment; a Pauline and Harold Price Endowment; NIH grants HL66389, P50 HL52319, and HL71140; the Cardiac Arrhythmia Research Enhancement Support Group Inc. (CARES), and the Ralph M. Parsons Foundation, Los Angeles, Calif. We thank Ning-Ning Chai, PhD, Gina Su, Avile McCullen, Szu-Cheng (Eric) Lin, and Elaine Lebowitz for their assistance and C. Thomas Peter, MD, for his support.

References

1. Cao J-M, Fishbein MC, Han JB, Lai WW, Lai AC, Wu T-J, Czer L, Wolf PL, Denton TA, Shintaku IP, Chen P-S, Chen LS. Relationship between regional cardiac hyperinnervation and ventricular arrhythmia. *Circulation*. 2000;101:1960–1969.
2. Cao J-M, Chen LS, KenKnight BH, Ohara T, Lee M-H, Tsai J, Lai WW, Karagueuzian HS, Wolf PL, Fishbein MC, Chen P-S. Nerve sprouting and sudden cardiac death. *Circ Res*. 2000;86:816–821.
3. Miyauchi Y, Zhou S, Okuyama Y, Miyauchi M, Hayashi H, Hamabe A, Fishbein MC, Mandel WJ, Chen LS, Chen PS, Karagueuzian HS. Altered atrial electrical restitution and heterogeneous sympathetic hyperinnervation in hearts with chronic left ventricular myocardial infarction: implications for atrial fibrillation. *Circulation*. 2003;108:360–366.
4. Chang C-M, Wu T-J, Zhou S-M, Doshi RN, Lee M-H, Ohara T, Fishbein MC, Karagueuzian HS, Chen P-S, Chen LS. Nerve sprouting and sympathetic hyperinnervation in a canine model of atrial fibrillation produced by prolonged right atrial pacing. *Circulation*. 2001;103:22–25.
5. Zhou S, Cao JM, Tebb ZD, Ohara T, Huang HL, Omichi C, Lee MH, KenKnight BH, Chen LS, Fishbein MC, Karagueuzian HS, Chen P-S. Modulation of QT interval by cardiac sympathetic nerve sprouting and the mechanisms of ventricular arrhythmia in a canine model of sudden cardiac death. *J Cardiovasc Electrophysiol*. 2001;12:1068–1073.

6. Chen P-S, Chen LS, Cao JM, Sharifi B, Karagueuzian HS, Fishbein MC. Sympathetic nerve sprouting, electrical remodeling and the mechanisms of sudden cardiac death. *Cardiovasc Res*. 2001;50:409–416.
7. Levi-Montalcini R. The nerve growth factor: its role in growth, differentiation and function of the sympathetic adrenergic neuron. *Progress in Brain Research*. 1976;45:235–258.
8. Edwards RH, Rutter WJ, Hanahan D. Directed expression of NGF to pancreatic beta cells in transgenic mice leads to selective hyperinnervation of the islets. *Cell*. 1989;58:161–170.
9. Anton ES, Weskamp G, Reichardt LF, Matthew WD. Nerve growth factor and its low-affinity receptor promote Schwann cell migration. *Proc Natl Acad Sci U S A*. 1994;91:2795–2799.
10. Lockhart ST, Turrigiano GG, Birren SJ. Nerve growth factor modulates synaptic transmission between sympathetic neurons and cardiac myocytes. *J Neurosci*. 1997;17:9573–9582.
11. Perrone-Bizzozero NI, Cansino VV, Kohn DT. Posttranscriptional regulation of GAP-43 gene expression in PC12 cells through protein kinase C-dependent stabilization of the mRNA. *J Cell Biol*. 1993;120:1263–1270.
12. Hassankhani A, Steinhelper ME, Soonpaa MH, Katz EB, Taylor DA, Andrade-Rozental A, Factor SM, Steinberg JJ, Field LJ, Federoff HJ. Overexpression of NGF within the heart of transgenic mice causes hyperinnervation, cardiac enlargement, and hyperplasia of ectopic cells. *Dev Biol*. 1995;169:309–321.
13. Derby A, Engleman VW, Frierdich GE, Neises G, Rapp SR, Roufa DG. Nerve growth factor facilitates regeneration across nerve gaps: Morphological and behavioral studies in rat sciatic nerve. *Exp Neurol*. 1993;119:176–191.
14. Kirkness EF, Bafna V, Halpern AL, Levy S, Remington K, Rusch DB, Delcher AL, Pop M, Wang W, Fraser CM, Venter JC. The dog genome: survey sequencing and comparative analysis. *Science*. 2003;301:1898–1903.
15. Ikeda T, Yashima M, Uchida T, Hough D, Fishbein MC, Mandel WJ, Chen P-S, Karagueuzian HS. Attachment of meandering reentrant wave fronts to anatomic obstacles in the atrium. Role of the obstacle size. *Circ Res*. 1997;81:753–764.
16. Heid CA, Stevens J, Livak KJ, Williams PM. Real time quantitative PCR. *Genome Res*. 1996;6:986–994.
17. Meiri KF, Pfenninger KH, Willard MB. Growth-associated protein, GAP-43, a polypeptide that is induced when neurons extend axons, is a component of growth cones and corresponds to pp46, a major polypeptide of a subcellular fraction enriched in growth cones [published erratum appears in *Proc Natl Acad Sci U S A* 1986;83:9274]. *Proc Natl Acad Sci U S A*. 1986;83:3537–3541.
18. Fishbein MC, Maclean D, Maroko PR. The histopathologic evolution of myocardial infarction. *Chest*. 1978;73:843–849.
19. Huang MH, Friend DS, Sunday ME, Singh K, Haley K, Austen KF, Kelly RA, Smith TW. An intrinsic adrenergic system in mammalian heart. *J Clin Invest*. 1996;98:1298–1303.
20. Heumann R, Korsching S, Scott J, Thoenen H. Relationship between levels of nerve growth factor (NGF) and its messenger RNA in sympathetic ganglia and peripheral target tissues. *EMBO J*. 1984;3:3183–3189.
21. Korsching S, Thoenen H. Developmental changes of nerve growth factor levels in sympathetic ganglia and their target organs. *Dev Biol*. 1988;126:40–46.
22. Li JY, Kling-Petersen A, Dahlstrom A. GAP 43-like immunoreactivity in normal adult rat sciatic nerve, spinal cord, and motoneurons: axonal transport and effect of spinal cord transection. *Neuroscience*. 1993;57:759–776.
23. Korsching S, Thoenen H. Nerve growth factor in sympathetic ganglia and corresponding target organs of the rat: correlation with density of sympathetic innervation. *Proc Natl Acad Sci U S A*. 1983;80:3513–3516.
24. Kaye MP, Wells DJ, Tyce GM. Nerve growth factor-enhanced reinnervation of surgically denervated canine heart. *Am J Physiol*. 1979;236:H624–H628.
25. Hiltunen JO, Laurikainen A, Vakeva A, Meri S, Saarma M. Nerve growth factor and brain-derived neurotrophic factor mRNAs are regulated in distinct cell populations of rat heart after ischaemia and reperfusion. *J Pathol*. 2001;194:247–253.
26. Curtis R, Stewart HJ, Hall SM, Wilkin GP, Mirsky R, Jessen KR. GAP-43 is expressed by nonmyelin-forming Schwann cells of the peripheral nervous system. *J Cell Biol*. 1992;116:1455–1464.
27. Aigner L, Arber S, Kapfhammer JP, Laux T, Schneider C, Botteri F, Brenner HR, Caroni P. Overexpression of the neural growth-associated protein GAP-43 induces nerve sprouting in the adult nervous system of transgenic mice. *Cell*. 1995;83:269–278.
28. Aigner L, Caroni P. Absence of persistent spreading, branching, and adhesion in GAP-43–depleted growth cones. *J Cell Biol*. 1995;128:647–660.
29. Heumann R, Korsching S, Bandtlow C, Thoenen H. Changes of nerve growth factor synthesis in nonneuronal cells in response to sciatic nerve transection. *J Cell Biol*. 1987;104:1623–1631.
30. Scherer SS, Xu YT, Roling D, Wrabetz L, Feltri ML, Kamholz J. Expression of growth-associated protein-43 kD in Schwann cells is regulated by axon-Schwann cell interactions and cAMP. *J Neurosci Res*. 1994;38:575–589.

Mechanisms of Cardiac Nerve Sprouting After Myocardial Infarction in Dogs

Shengmei Zhou, Lan S. Chen, Yasushi Miyauchi, Mizuho Miyauchi, Saibal Kar, Simon Kangavari, Michael C. Fishbein, Behrooz Sharifi and Peng-Sheng Chen

Circ Res. published online May 27, 2004;
Circulation Research is published by the American Heart Association, 7272 Greenville Avenue, Dallas, TX 75231

Print ISSN: 0009-7330. Online ISSN: 1524-4571